Integrating muti-omics data to identify tissue-specific DNA methylation biomarkers for cancer risk

Yaohua Yang[1†*], Yaxin Chen[2†], Shuai Xu[3], Xingyi Guo[3], Guochong Jia[3], Jie Ping[3], Xiang Shu[4], Tianying Zhao[3], Fangcheng Yuan[3], Gang Wang[2], Yufang Xie[2], Hang Ci[2], Hongmo Liu[2], Yawen Qi[2], Yongjun Liu[5], Dan Liu[2], Weimin Li[2], Fei Ye[6], Xiao-Ou Shu[3], Wei Zheng[3], Li Li[7], Qiuyin Cai[3*], Jirong Long[3*]

***** Corresponding authors contact information:

Dr. Yaohua Yang, Center for Public Health Genomics, School of Medicine, University of Virginia. Address: 560 Ray C. Hunt Dr, Rm 4408, Charlottesville, VA 22903. Email: vta8we@virginia.edu

Dr. Qiuyin Cai, Division of Epidemiology, Department of Medicine, Vanderbilt University Medical Center. Address: 1161 21st Avenue South, MCN B-2104, Nashville, TN, 37232. Email: qiuyin.cai@vanderbilt.edu

Dr. Jirong Long, Division of Epidemiology, Department of Medicine, Vanderbilt University Medical Center. Address: 2525 West End Avenue, Suite 800, Nashville, TN, 37203. Email: jirong.long@vumc.org

† These authors contribute equally to this work

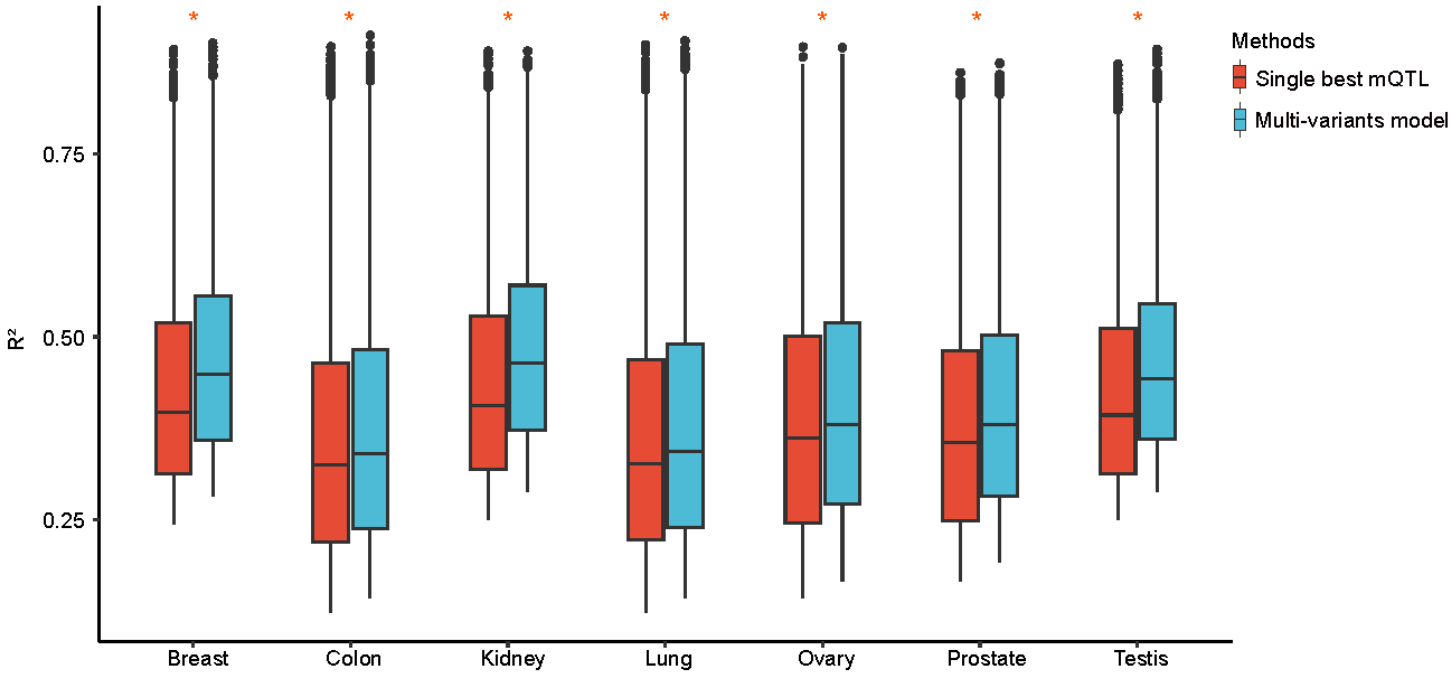

Supplementary Fig. 1. Prediction performance of models established by the present study and mQTLs. CpGs that could be reliably predicted (R>0.10 and *P*<0.05) by both our prediction models and mQTLs were used for comparison. The number of such CpGs is n=24,604 for breast tissue, n=85,285 for colon tissue, n=31,296 for kidney tissue, n=87,987 for lung tissue, n=76,161 for ovary tissue, n=51,193 for prostate tissue, and n=24,297 for testis tissue. Boxes represent the interquartile range, black bars are medians, whiskers extend at most 1.5 times the interquartile range, and outliers are shown individually. Red asterisk denotes *P*≈0 in two-sided paired t-test. mQTL, methylation quantitative trait loci. Source data are provided as a Source Data file.

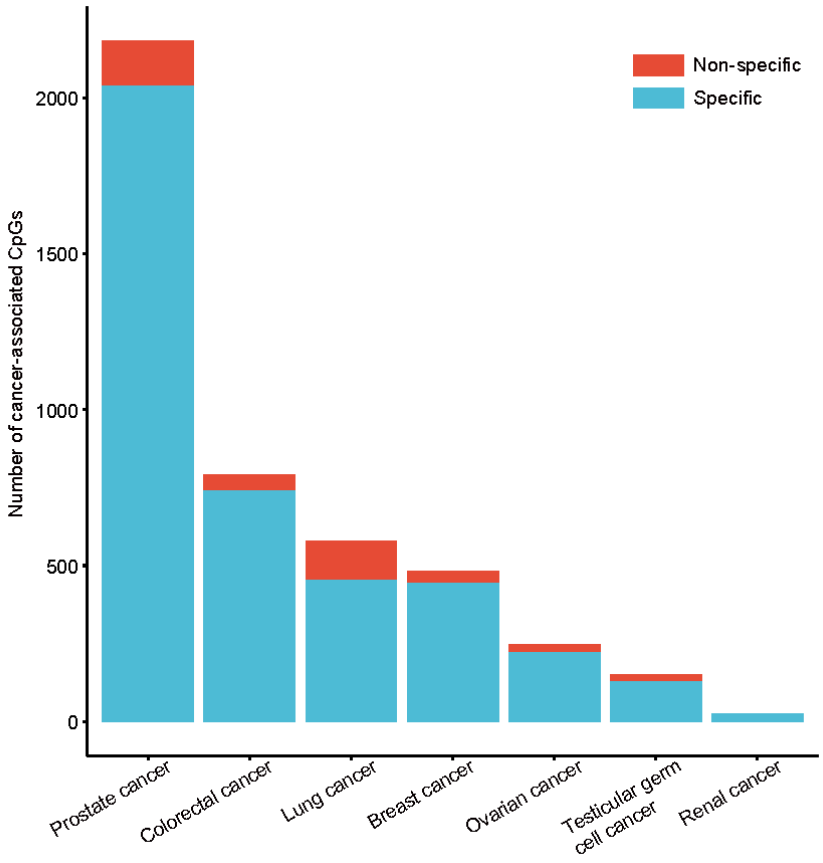

Supplementary Fig. 2. **Tissue-specificity of cancer-associated CpGs**. For each cancer, association analyses of genetically predicted DNA methylation (DNAm) with cancer risk were performed using SPrediXcan and significant associations were identified at Bonferroni-corrected two-side $P<0.05$, corresponding to 4.93×10^{-7} for breast cancer (n=101,497 CpGs tested; n=539,198 subjects), 2.53×10^{-7} for colorectal cancer (n=197,947 CpGs tested; n=254,791 subjects), 3.98×10^{-7} for renal cell cancer (n=125,745 CpGs tested; n=31,190 subjects), 2.55×10^{-7} for lung cancer (n=195,764 CpGs tested; n=887,170 subjects), 2.66×10^{-7} for ovarian cancer (n=187,911 CpGs tested; n=70,668 subjects), 3.28×10^{-7} for prostate cancer (n=152,341 CpGs tested; n=944,762 subjects), and 4.22×10^{-7} for testicular germ cell cancer (n=118,568 CpGs tested; n=28,135 subjects). CpGs that were exclusively associated with a particular cancer at Bonferroni-corrected $P<0.05$ are considered tissue specific. Source data are provided as a Source Data file.

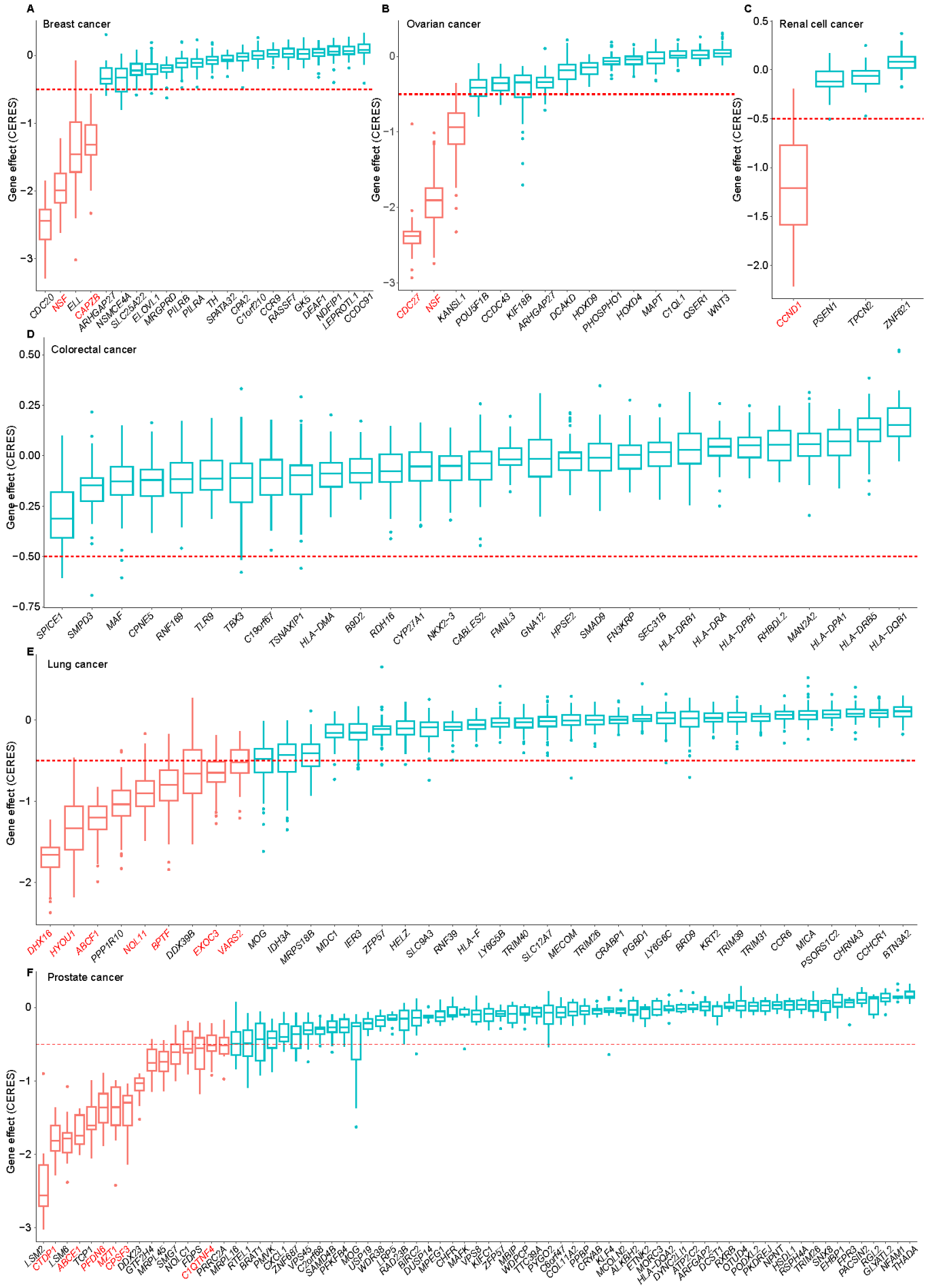
A
Breast cancer
Gene effect (CERES)
CDC20 NSF EIL CAPZB ARHGAP27 NSMCE4A SLC25A22 ELOVL1 MRGPRD PILRB PILRA TH SPATA32 CPA2 C1orf210 CCR9 RASSF7 GK5 DEAF1 NDFIP1 LEPROTL1 CCDC91
B
Ovarian cancer
Gene effect (CERES)
CDC27 NSF KANSL1 POU5F1B CCDC43 KIF18B ARHGAP27 DCAKD HOXD9 PHOSPHO1 HOXD4 MAPT C1QL1 GSER1 WNT3
C
Renal cell cancer
Gene effect (CERES)
CCND1 PSEN1 TPCN2 ZNF621
D
Colorectal cancer
Gene effect (CERES)
SPICE1 SMPD3 MAF CPNE5 RNF169 TLR9 TBX3 C19orf67 TSNAXIP1 HLA-DMA BBD2 RDH16 CYP27A1 NKX2-3 CABLES2 FMNL3 GNA12 HPSE2 SMAD9 FN3KRP SEC31B HLA-DRB1 HLA-DRA HLA-DPB1 RHBDL2 MAN2A2 HLA-DPA1 HLA-DRB5 HLA-DQB1
E
Lung cancer
Gene effect (CERES)
DHX16 HYOU1 ABCF1 PPP1R10 NOL11 BPTF DDX39B EXOC3 VARS2 MOG IDH3A MRPS18B MDC1 IER3 ZFP57 HELZ SLC9A3 RNF39 HLA-F LY6G5B TRIM40 SLC12A7 MECOM TRIM26 CRABP1 PGBD1 LY6G6C BRD9 KRT2 TRIM39 TRIM31 CCR6 MICA PSORS1C2 CHRNA3 CCHCR1 BTN3A2
F
Prostate cancer
Gene effect (CERES)
LSM2 CTDP1 LSM6 ABCE1 TCP1 PFDN6 MTF1 CPSF3 DDX23 GTF2H4 MRPL45 SMG7 NOL1C1 FDPS C1QTNF4 PRRC2A MRPL16 RTEL1 BRAT1 PMVK CXCL1 ZNF687 VPS45 C20orf85 SAMD4B PFKFB4 MOG USP19 WDR38 LRP5 RAD23B BIRC2 DUSP14 MPEG1 CHER MAPK VPS8 KIFC1 ZFP57 MBIP WDPCP TTC39A PYGO2 C8orf47 COL11A2 PPRP CRYAB KLF4 MCOLN2 ALKBH2 FTMT2 MORC3 HLA-DQA2 DYNC2LI1 ATP2C2 ARFGAP2 DCST1 RXRB OTUD4 PODXL2 PKDREJ NPNT HSDL1 RSPH4A TRIM26 SNX8 EHBP1 PACSIN2 RGL2 GLYATL2 NFAM1 THADA

Supplementary Fig. 3. Essential roles in cell proliferation of genes associated with cancer-associated CpGs. Boxplots show effects of genes on cell proliferation using experimental data from Clustered Regularly Interspaced Short Palindromic Repeats (CRISPR) screens. Boxes represent the interquartile range, black bars are medians, whiskers extend at most 1.5 times the interquartile range, and outliers are shown individually. The dashed red line in each plot denotes the essentiality threshold of median CERES values<-0.50. Genes shown in CpG-gene-cancer trios revealed by downstream analyses (see **Methods**) are highlighted in red. **A**, breast cancer (n=48 cell lines). **B**, ovarian cancer (n=57 cell lines). **C**, renal cell cancer (n=32 cell lines). **D**, colorectal cancer (n=57 cell lines). **E**, lung cancer (n=114 cell lines). **F**, prostate cancer (n=10 cell lines). Source data are provided as a Source Data file.

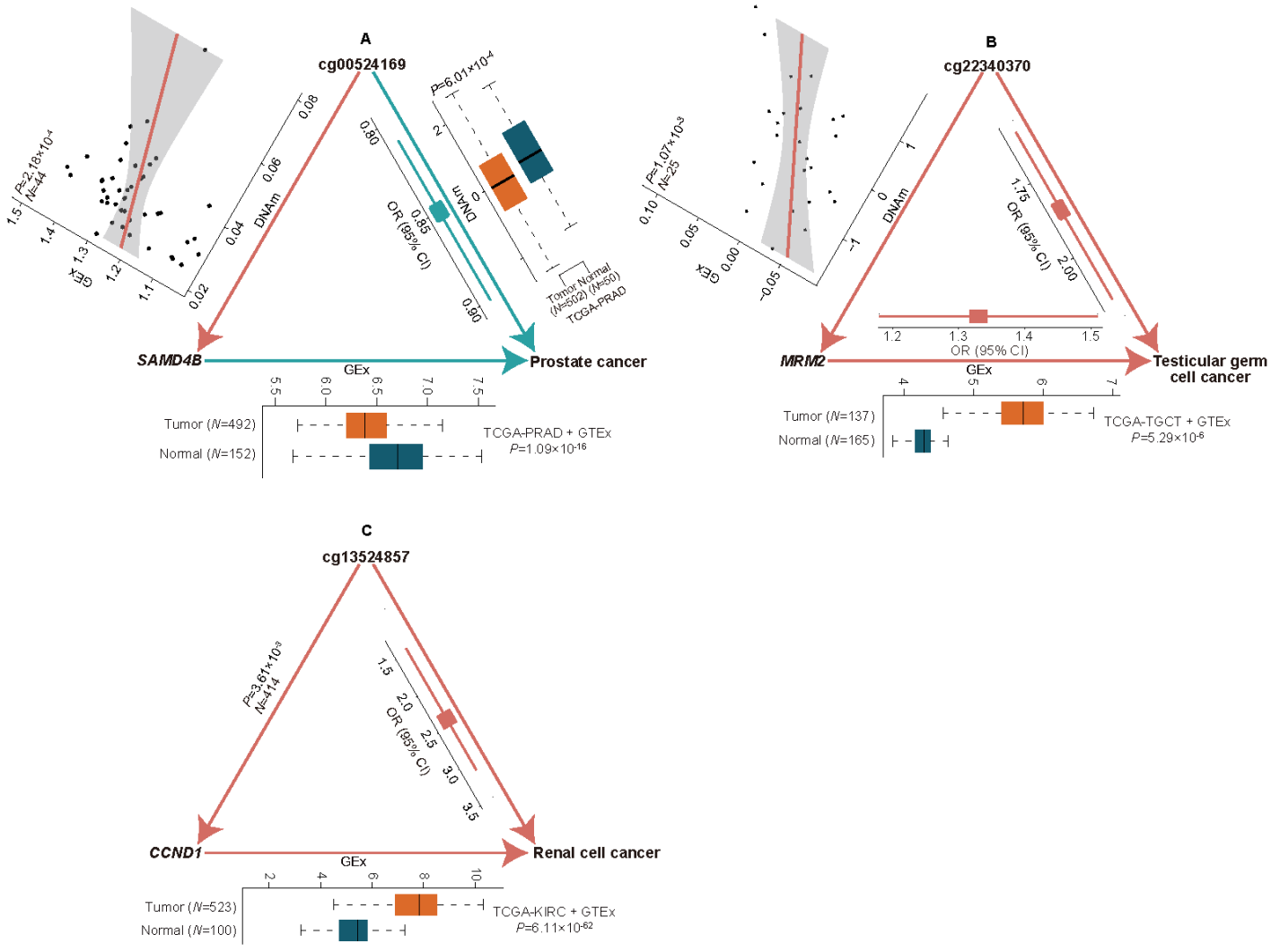

Supplementary Fig. 4. **Additional examples of CpG-gene-cancer trios suggesting DNA methylation influencing cancer risk by modulating *cis*-gene expression**. Association analyses of genetically predicted DNA methylation (DNAm) or gene expression (GEx) with cancer risk were performed using SPrediXcan. Differential DNAm or GEx analyses were conducted using linear mixed models. Association analyses between DNAm and GEx were performed using linear regression. Red arrows, lines, and blocks denote positive associations, while green ones denote negative associations. All statistical tests were two-sided and multiple comparisons were Bonferroni- or false discovery rate (FDR)-adjusted. The odds ratio (OR) and 95% confidence interval (CI) for cancer risk per standard deviation (SD) increase in genetically predicted DNAm or GEx are displayed as a block with error bands. In

boxplots, boxes represent the interquartile range, black bars are medians, and whiskers extend at most 1.5 times the interquartile range. In the scatter plot displaying the association between DNAm and GEx, directly measured DNAm and GEx values after quantile- and inverse-normalization are presented. n, number of samples, TCGA, The Cancer Genome Atlas; GTEx, Gene-Tissue Expression consortium; PRAD, prostate adenocarcinoma; TGCT, testicular germ cell tumors; KIRC, kidney renal clear cell carcinoma. **A**, DNAm at cg00524169 may decrease prostate cancer risk by promoting the expression of *SAMD4B*. The sample size was 552 for tumor-normal differential DNAm analyses, 44 for DNAm-GEx correlation analyses, 644 for tumor-normal differential GEx analyses, and 944,762 for association analyses of predicted DNAm and GEx with prostate cancer risk, respectively. **B**, DNAm at cg22340370 may elevate testicular germ cell cancer risk by promoting the expression of *MRM2*. The sample size was 25 for DNAm-GEx correlation analyses, 302 for tumor-normal differential GEx analyses, and 28,135 for association analyses of predicted DNAm and GEx with testicular germ cell cancer risk, respectively. **C**, DNAm at cg13524857 may increase renal cell cancer risk by promoting the expression of *CCND1*. The sample size was 414 for DNAm-GEx correlation analyses, 623 for tumor-normal differential GEx analyses, and 31,190 for association analyses of predicted DNAm and GEx with renal cell cancer risk, respectively. Source data are provided as a Source Data file.